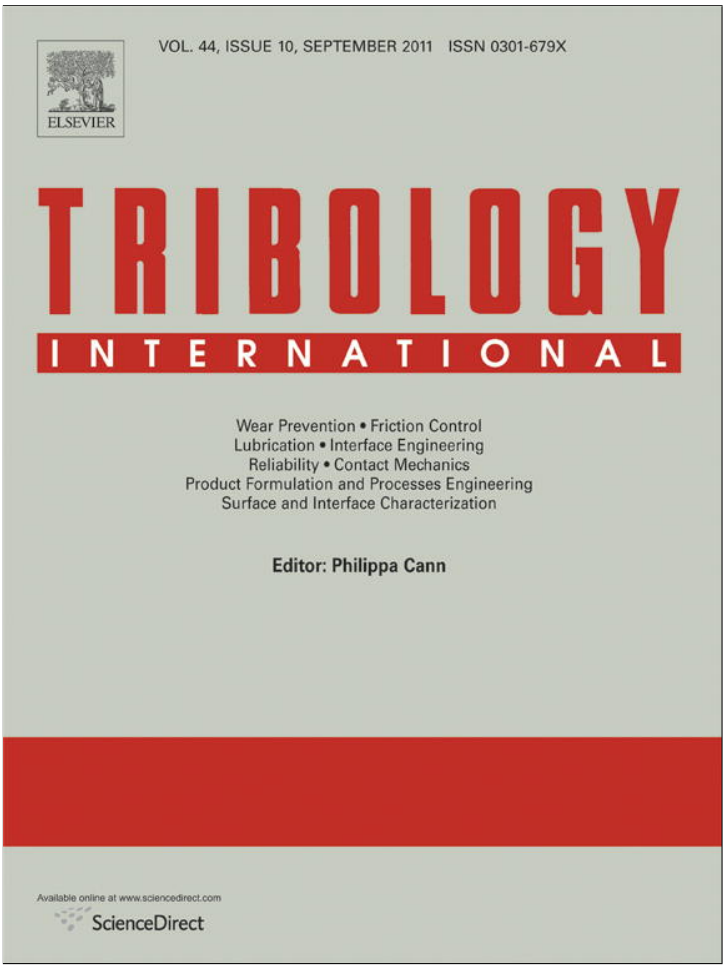

Tribology International 44 (2011) 1089–1099

Contents lists available at ScienceDirect

Tribology International

journal homepage: www.elsevier.com/locate/triboint

Approximate analytical solution to Reynolds equation for finite length journal bearings

Gustavo G. Vignolo [a,b,c,*], Daniel O. Barilá [c], Lidia M. Quinzani [a]

[a] Planta Piloto de Ingeniería Química (PLAPIQUI), UNS-CONICET, CC 717 Bahía Blanca, Argentina
[b] Engineering Department, Universidad Nacional del Sur (UNS), Alem 1253, 8000, Bahía Blanca, Argentina
[c] Universidad Nacional de la Patagonia San Juan Bosco (UNPSJB), Ruta Prov. No. 1, km. 4, 9005 Comodoro Rivadavia, Argentina

ARTICLE INFO

Article history:
Received 11 November 2010
Received in revised form
16 March 2011
Accepted 22 March 2011
Available online 5 May 2011

Keywords:
Regular perturbation
Hydrodynamic lubrication
Reynolds equation
Journal bearings

ABSTRACT

The understanding of the behavior of hydrodynamic bearings requires the analysis of the fluid film between two solid surfaces in relative motion. The differential equation that governs the movement of this fluid, called the Reynolds equation, arises from the integration over the film thickness of the continuity equation, previously combined with the Navier–Stokes equation. An order of magnitude analysis, which is based on the relative value of the dimensions of the bearing, produces two dimensionless numbers that govern the behavior of the system: the square of the aspect ratio, length over diameter $(L/D)^2$, and the eccentricity ratio (η). An analytical solution of the Reynolds equation can only be obtained for particular situations as, for example, the isothermal flow of Newtonian fluids and values of $L/D \to 0$ or $L/D \to \infty$. For other conditions, the equation must be solved numerically.

The present work proposes an analytical approximate solution of the Reynolds equation for isothermal finite length journal bearings by means of the regular perturbation method. $(L/D)^2$ is used as the perturbation parameter. The novelty of the method lays in the treatment of the Ocvirk number as an expansible parameter.

The zero-order solution of the Reynolds equation (obtained for $L/D \to 0$), which matches the Ocvirk solution, may be used to describe the behavior of finite length journal bearings, up to $L/D \sim 1/8$–$1/4$, and relatively small eccentricities. The first-order solution obtained with the proposed method gives an analytical tool that extends the description of pressure and shear-stress fields up to $L/D \sim 1/2$ and $\eta \sim 1/2$ (or combinations of larger eccentricities with smaller aspect ratios, or vice versa). Moreover, the friction force and load-carrying capacity are accurately described by the proposed method up to $L/D \sim 1$ and η very near to 1.

1. Introduction

The understanding of hydrodynamic lubrication began in the 19th century and many advances have been done since then [1]. Nevertheless, the exact analytical solution of the governing equations is still not possible in most applications, and numerical methods are required to solve them. However, it is always useful to have analytical solutions, even approximate ones, to understand the overall behavior of the system and the dominant effects.

When the thin-film lubrication approximation is considered, the pressure in the lubricant film is described by the Reynolds equation [2]. This equation is obtained by integrating the continuity equation, previously combined with the Navier–Stokes equations, into the film thickness. The result is a nonhomogeneous partial differential equation of elliptical type that, in general, requires considerable numerical effort to be solved. However, approximate solutions have been obtained using electrical analogies, mathematical summations, relaxation methods, and numerical and graphical methods [1,3,4].

The present work is focused on journal bearings (JBs). The hydrodynamically lubricated JBs are bearings that develop load-carrying capacity due to the relative motion of two quasi-concentric cylinders separated by a fluid film [1]. The two most widely used approximations of the Reynolds equation for this type of bearings are the ones known as the "infinitely short journal bearing" (ISJB) [5] and the "infinitely long journal bearing" (ILJB) [6], depending on the derivative of the pressure that is not considered. In both these cases, the Reynolds equation reduces to a linear ordinary differential equation for which closed form analytical solutions exist. The significance of the ISJB and ILJB solutions lie not only in the fact that they are analytical but also in that they indicate trends, and often establish upper and lower limits to a JB performance [3]. Most of the attempts that have been done to solve the complete Reynolds equation for finite length JBs contemplate these ideal limit cases. For example, one

* Corresponding author at: Planta Piloto de Ingeniería Química (PLAPIQUI), UNS-CONICET, CC 717 Bahía Blanca, Argentina.
E-mail address: gvignolo@plapiqui.edu.ar (G.G. Vignolo).

0301-679X/$ - see front matter © 2011 Elsevier Ltd. All rights reserved.
doi:10.1016/j.triboint.2011.03.020

Nomenclature

D	journal bearing diameter, $D=2R$
F	magnitude of the load-carrying capacity
F_f	friction force, $F_f=fF$
F_x	X-component of the load-carrying capacity
F_y	Y-component of the load-carrying capacity
H	film thickness, $H=c+e\cos(\theta)$
L	journal bearing length
O	Ocvirk number, $O=\frac{\mu U}{RP_p}\left(\frac{R}{c}\right)^2\left(\frac{L}{R}\right)^2$
O_0	zero-order Ocvirk number
O_1	first-order Ocvirk number
P	pressure
P_{EXT}	external pressure
P_p	projected load
P_{REF}	characteristic pressure
R	journal bearing radius
S	Sommerfeld number, $S=\frac{\mu U}{RP_p}\left(\frac{R}{c}\right)^2$
T	dimensionless shear stress, $T=-\frac{\partial u}{\partial y}\Big\vert_h=\tau\Big\vert_{\frac{hc}{\mu U}}$
U	surface journal velocity—characteristic tangential velocity
V	characteristic radial velocity
V_Θ	tangential velocity
V_y	radial velocity
V_z	axial velocity
W	characteristic axial velocity
X	tangential coordinate
Y	radial coordinate
Z	axial coordinate
c	journal bearing clearance
e	eccentricity
f	friction coefficient
h	dimensionless film thickness $h=\frac{H}{c}=1+\eta\cos(\pi\Theta)$
p	dimensionless pressure, $p=\frac{P-P_{EXT}}{P_p}$
p_0	zero-order dimensionless pressure
p_1	first-order dimensionless pressure
p'	dimensionless pressure, $p'=\frac{P-P_{EXT}}{P_{REF}}$
u	dimensionless tangential velocity, $u=\frac{V_\Theta}{U}$
u_c	dimensionless linear tangential velocity, $u_c=\frac{U}{h}$
v	dimensionless radial velocity, $v=\frac{V_y}{V}$
w	dimensionless axial velocity, $w=\frac{V_z}{W}$
y	dimensionless radial coordinate, $y=\frac{Y}{c}$
z	dimensionless axial coordinate, $z=\frac{Z}{L}$
Θ	dimensionless tangential coordinate, $\Theta=\frac{\theta}{\pi}=\frac{X}{R\pi}=\frac{x}{\pi}$
ε	perturbation parameter, $\varepsilon=\left(\frac{L}{D}\right)^2$
η	eccentricity ratio, $\eta=\frac{e}{c}$
μ	fluid viscosity
τ	shear stress

approach is the one that assumes the existence of a homogeneous solution plus a particular one given by the ILJB solution [3]. In that case, the homogeneous solution, if obtainable, may be regarded as a 'correction factor' of the ILJB for finite length JBs [3,7].

Another approach frequently used to solve the Reynolds equation contemplates the use of asymptotic methods [8–10]. These methods have been used to approximate the solution to fluid film lubrication problems like those of slider, step, partial, and JBs. For example, asymptotic results have been obtained for infinitely long slider and step squeeze-film bearings using different asymptotic expansions to take into account the effects of the trailing edge and to reach smaller values of the squeeze and bearing numbers [11–14]. Infinitely long slider bearings and slider bearings with a discontinuity in the film slope at high bearing numbers have also been analyzed with similar methods [15,16]. The general finite width gas slider bearing has also been studied in order to find a formal explicit uniformly valid asymptotic representation of the pressure with a low order error over the entire bearing [17–19]. In the case of short slider bearings, the descriptions have been done by rectifying the infinitely short bearing theory and performing an asymptotic analysis to correct the pressure field near both, the leading and the trailing edges of the slider [20,21], and by solving an Euler–Lagrange equation using a small aspect ratio singular perturbation approach [22]. The infinitely short bearing theory has been also applied to cylindrical partial-arc short bearings using a matched asymptotic perturbation method to correct the inaccuracies caused by the azimuthal edge pressure boundary conditions [20,21,23]. The finite length JB with high-eccentricity has been analyzed in terms of inner and outer asymptotic expansions to get the pressure distribution inside the fluid film, load-carrying capacity, and frictional loss [24]. Furthermore, several authors have contemplated the effect of nonzero inertia and curvature, not present in the Reynolds' equation, on the ILJB using different series expansions methods [25–29]. Regular perturbation series expansions have been applied to extend the range of applicability of the ISJB and to quantify the accuracy of this ideal limit solution [21]. When all the previously mentioned methods and approaches are considered, one thing that has to be kept in mind is that the Reynolds equation is a multi-parameter equation, and consequently, the different expanded solutions present limitations and restrictions associated to the chosen parameters.

The constant development towards higher speed, higher performance, but smaller size machinery has established the trend to the use of shorter bearings [30]. For that reason, the ISJB approximation has received much attention over the years. Furthermore, if an isothermal and incompressible Newtonian fluid is considered, this approximation yields a simple pressure field, which is a function of both, the tangential and axial coordinates, and satisfies all pressure boundary conditions [1,3]. This solution is frequently applied in the areas of rotor-bearing dynamics, dampers, and shaft seals, even though the accuracy of the ISJB solution depends on how close the real conditions are to the assumed ones. In that sense, the nonzero aspect ratio (length over diameter) and eccentricity are the most important factors that deviate the real solution from the ISJB approximation [21,31]. In order to get more accurate results, specific analytic developments have been carried out to perform dynamic analyses. In general, these developments use different combinations of short and long bearing solutions [32,33].

The purpose of the present work is to provide a new analytical solution valid to finite length JBs obtained as an extension of the ISJB approximation by means of the regular perturbation method. In the following section, the governing equations as well as the resulting equations from the order of magnitude analysis are presented. Then, the proposed approach to the regular perturbation method is discussed, and finally the predicted variables are compared to the results from numerical solutions as well as other analytical approaches.

2. Governing equations

Fig. 1 displays a scheme of the JB together with the associated coordinate system and some dimensions. The journal, of radius R, turns inside a bearing of length L at an angular speed Ω. The loci

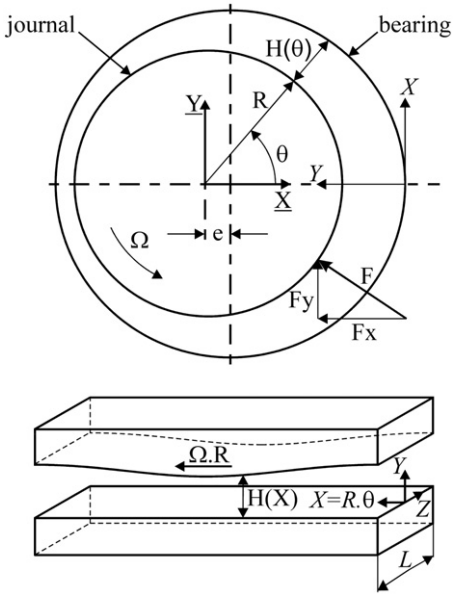

Fig. 1. Geometry and system of coordinates.

of the journal and the bearing are separated by a distance, e, called eccentricity. The maximum value that e can reach, c, is the difference between bearing and journal radii. The gap between them, H, is fully filled with an incompressible fluid, the lubricant. Although both, journal and bearing, are cylinders, the flow of the lubricant in the gap can be studied in rectangular coordinates $\{X,Y,Z\}$, ignoring the curvature, because R is several orders of magnitude larger than c. Dimensionless coordinates Θ, y, and z are defined by means of the characteristic values πR, c, and L as

$$\Theta = \frac{X}{\pi R}, \quad y = \frac{Y}{c}, \quad z = \frac{Z}{L} \tag{1}$$

For isothermal flow, the dimensionless variables of interest are the tangential velocity, u, axial velocity, w, radial velocity, v, and pressure, p', defined as

$$u = \frac{V_\Theta}{U}, \quad v = \frac{V_y}{V}, \quad w = \frac{V_z}{W}, \quad p' = \frac{P - P_{EXT}}{P_{REF}} \tag{2}$$

where U, V, W, and P_{REF} are the characteristic values of the corresponding variables.

The dimensionless mass balance equation:

$$0 = \frac{U}{\pi R}\frac{\partial u}{\partial \Theta} + \frac{V}{c}\frac{\partial v}{\partial y} + \frac{W}{L}\frac{\partial w}{\partial z} \tag{3}$$

determines the values of $V = Uc/R$ and $W = UL/R$ if the three terms are of similar order of magnitude.

The dimensionless momentum conservation equations can be largely simplified neglecting the terms that are of an order of magnitude c/R, since this ratio normally has values of the order of 1/1000. Accordingly, the final expressions of the Θ-, y- and z-direction momentum balances are, respectively

$$0 = -\frac{P_{REF}}{\pi R}\frac{\partial p'}{\partial \Theta} + \mu\frac{U}{c^2}\frac{\partial^2 u}{\partial y^2} \quad 0 = -\frac{P_{REF}}{c}\frac{\partial p'}{\partial y} + \mu\frac{V}{c^2}\frac{\partial^2 v}{\partial y^2}$$
$$0 = -\frac{P_{REF}}{L}\frac{\partial p'}{\partial z} + \mu\frac{W}{c^2}\frac{\partial^2 w}{\partial y^2} \tag{4}$$

The main assumption of the ISJB approximation, known as the "Ocvirk solution" [5], is that the pressure gradient in the Θ-direction can be neglected when compared to the axial one. This means that the tangential speed profile should be linear, like in Couette flow, and that P_{REF} can be estimated from the z-direction momentum balance and defined as

$$P_{REF} = \frac{\mu U}{R}\left(\frac{R}{c}\right)^2\left(\frac{L}{R}\right)^2 \tag{5}$$

In this case, the dimensionless mass and momentum equations take the following form:

$$0 = \frac{1}{\pi}\frac{\partial u}{\partial \Theta} + \frac{\partial v}{\partial y} + \frac{\partial w}{\partial z} \tag{6}$$

$$0 = -\frac{1}{\pi}\left(\frac{L}{R}\right)^2\frac{\partial p'}{\partial \Theta} + \frac{\partial^2 u}{\partial y^2} \quad 0 = -\frac{\partial p'}{\partial y} + \left(\frac{c}{L}\right)^2\frac{\partial^2 v}{\partial y^2} \quad 0 = -\frac{\partial p'}{\partial z} + \frac{\partial^2 w}{\partial y^2} \tag{7}$$

On the other hand, the main assumption of the ILJB, known as the "Sommerfeld solution" [6], is that the axial pressure gradient is much smaller than the tangential one. No axial speed profile is then expected. The value of P_{REF} can be then calculated from the Θ-direction momentum equation, and defined as $P_{REF} = \mu U/R(R/c)^2$. In both, the ISJB and the ILSB cases, the pressure gradient in the radial direction can be neglected because the momentum conservation equations in the y-direction are $(c/R)^2$ or $(c/L)^2$ times smaller, respectively, than the equations in the other two directions.

2.1. Reynolds equation

The so called Reynolds equation [2] is obtained combining the mass and momentum balances and integrating the mass balance within the thickness of the film considering non-slip boundary conditions over the walls for all velocity components. If h is the dimensionless gap, defined as $h = H/c$, the dimensionless expression of the complete Reynolds equation is

$$\frac{dh}{d\Theta} = \frac{1}{6\pi}\left(\frac{L}{R}\right)^2\frac{\partial}{\partial \Theta}\left(h^3\frac{\partial p'}{\partial \Theta}\right) + \frac{\pi}{6}h^3\frac{\partial^2 p'}{\partial z^2} \tag{8}$$

when the dimensionless pressure P_{REF} is defined according to Eq. (5) for short JBs.

Clearly, the use of the ISJB hypothesis in Eq. (8) makes the term that includes the $(L/R)^2$ factor negligible. The resulting simplified equation has only two terms and it is analytically solvable using appropriate boundary conditions for the pressure. It is clear from the comments above that an extension of the two ideal cases (ISJB and ILJB) to finite length JBs should consider the fact that the order of magnitude of pressure changes with aspect ratio.

2.2. Sommerfeld and Ocvirk numbers

Traditionally, the behavior of JBs has been related to the Bearing or Sommerfeld number [1,6], S, or the capacity or Ocvirk number [5,34], $S(L/D)^2$. In the following sections, a slightly modified definition of the Ocvirk number, O, is used, in which the square of the length-to-diameter ratio is replaced by the square of the length-to-radius ratio. The resulting used expressions are

$$S = \frac{\mu U}{RP_p}\left(\frac{R}{c}\right)^2, \quad O = S\left(\frac{L}{R}\right)^2 \tag{9}$$

where P_p is a mean pressure defined as the ratio between the load-carrying capacity and the projected area, $2RL$. Thus, the Sommerfeld number represents the ratio between P_{REF} for ILJBs and the mean pressure P_p, while the Ocvirk number corresponds to the ratio between P_{REF} for ISJBs (Eq. (5)) and P_p. Traditionally, these numbers are defined using the shaft speed in RPS [1,3,35], which introduces a factor of 2π with respect to the definitions of both S and O in Eq. (9).

If the Sommerfeld and the Ocvirk numbers are introduced in the Reynolds equation, the dimensionless pressure changes from

p' to p, which is given by

$$p = \frac{P - P_{EXT}}{P_p} \tag{10}$$

and Eq. (8) becomes

$$O\frac{dh}{d\Theta} = S\left(\frac{L}{R}\right)^2 \frac{dh}{d\Theta} = \frac{1}{6\pi}\left(\frac{L}{R}\right)^2 \frac{\partial}{\partial\Theta}\left(h^3\frac{\partial p}{\partial\Theta}\right) + \frac{\pi}{6}h^3\frac{\partial^2 p}{\partial z^2} \tag{11}$$

This equation shows that S must tend to infinity as $(L/R)^2$ tends to zero in order to keep the equality between the two dominant terms. Consequently, when applied to ISJBs, the solution of the two remaining terms of Eq. (11) can only be used for bearings working at very high Sommerfeld numbers. Furthermore, since the larger the Sommerfeld number, the smaller the eccentricity [1], when a bearing works at high Sommerfeld number, the eccentricity tends to zero, and vice versa. Then, the ISJB's solution is also accurate for very small eccentricities.

3. Finite length JBs and proposed analytical solution

Although in their work, Dubois and Ocvirk [5] suggested that the ISJB approximation could be used for aspect ratios up to one, the following research demonstrated that this assumption is only justified for bearings with L/D smaller than $\sim 1/8$, for all eccentricities. In practice the assumption is used for L/D up to $\sim 1/2$ and eccentricities up to 0.75 [35].

The analysis of finite length JBs may be done by "shortening" the ILJB or "lengthening" the ISJB. The former approach can be applied considering an edge effect on the extremes of the bearing with a thickness of order of magnitude R/L. Each edge is treated as a "boundary layer" by means of functional analysis, and the solution of this zone is then matched to that of the "center zone" of the bearing [7].

The extension of the solution from ISJBs to finite length bearings can be done by applying the Regular Perturbation Method [36]. Perturbation approaches have historically been viewed as a viable method for analyzing higher order effects. Buckholz and Hwang [21] proposed an analysis of the Reynolds equation for short bearings by introducing a regular perturbation expansion for the pressure. The mathematical problem was determined by an ordering of the pressure terms of the series according to powers of the bearing aspect ratio. The expression of the zero-order solution is the Ocvirk solution while higher order terms in the pressure expansion are determined by a recursion formula. However, while the correction terms in this series should decrease in importance as the order increases, this does not happen neither near the minimum gap nor at values of eccentricity close to unity. This occurs because this is a multiple parameter problem. To solve it, the authors proposed a more stringent scaling of the Reynolds lubrication equation considering the aspect ratio and the eccentricity parameter to be in the same order of magnitude. Consequently, they pointed out that the Poiseuille flow component in the sliding direction becomes important near the minimum gap region when the eccentricity is sufficiently large for any given value of aspect ratio.

However, if only one length scale is considered, like in the first part of the work of Buckholz and Hwang [21], more than one variable must be taken in account in the series expansion to keep in balance the order of magnitude of the terms of the differential equations. For example, in addition to the pressure, other authors [25,29] have expanded the stream function or the Reynolds number, but none of these approaches were applied to ISJBs.

In the present paper, an extension of the short bearing approximation to finite length JBs is proposed using a regular perturbation method with the perturbation parameter, ε, defined as

$$\varepsilon = \left(\frac{L}{D}\right)^2 \tag{12}$$

where D is the diameter of the journal ($D=2R$). The difference with respect to previous methods is that the balance between the terms of the Reynolds equation is kept by expanding not only the pressure but also the Ocvirk number. In that way, the resulting pressure field should be able to describe JBs with higher eccentricities and higher aspect ratios than previous methods in which only the pressure was expanded. Thus,

$$p = p_0 + \left(\frac{L}{D}\right)^2 p_1 + \mathcal{O}\left(\frac{L}{D}\right)^4 \rightarrow p = p_0 + \varepsilon p_1 + \mathcal{O}(\varepsilon^2) \tag{13}$$

and

$$O = O_0 + \left(\frac{L}{D}\right)^2 O_1 + \mathcal{O}\left(\frac{L}{D}\right)^4 \rightarrow O = O_0 + \varepsilon O_1 + \mathcal{O}(\varepsilon^2) \tag{14}$$

Introducing these expansions into the Reynolds equation (Eq. (11)) and keeping the terms up to order ε, gives

$$(O_0 + \varepsilon O_1)\frac{dh}{d\Theta} = \frac{2}{3\pi}\varepsilon\frac{\partial}{\partial\Theta}\left(h^3\frac{\partial p_0}{\partial\Theta}\right) + \frac{\pi}{6}h^3\frac{\partial^2(p_0+\varepsilon p_1)}{\partial z^2} \tag{15}$$

To solve this equation, the dimensionless gap, h, can be calculated with

$$h = \frac{H}{c} = 1 + \eta\cos(\pi\Theta) \tag{16}$$

where η is the eccentricity ratio defined as

$$\eta = \frac{e}{c} \tag{17}$$

The zero-order solution (p_0 and O_0) is the solution of the ISJB ($L/D=0$), known as the Ocvirk solution. This solution gives the pressure field

$$p_0 = 3O_0\left[\frac{1}{4} - z^2\right]\frac{\eta\sin(\pi\Theta)}{\left[1+\eta\cos(\pi\Theta)\right]^3} \tag{18}$$

The boundary conditions used to obtain this equation are $p_0=0$ at $z=-1/2$, and $\partial p_0/\partial z=0$ at half the length ($z=0$). This pressure field automatically satisfies the conditions along the azimuthal boundaries for a JB, that is, $p_0=0$ at $\Theta=0$ and $\Theta=2$.

The first-order solution of Eq. (15) gives

$$p_1 = \frac{2(\alpha_1\eta\sin(\pi\Theta) + \alpha_2\eta^2\sin(2\pi\Theta) + 1/4\alpha_2\eta^3\sin(3\pi\Theta))}{\alpha_3\cos(\pi\Theta) + \alpha_4\cos(2\pi\Theta) + \alpha_5\cos(3\pi\Theta) + \alpha_6\cos(4\pi\Theta) + \alpha_7\cos(5\pi\Theta) + \alpha_8} \tag{19}$$

where

$$\begin{aligned}
&\alpha_1 = -\frac{O_0}{4}(5-24z^2+16z^4)(2-7\eta^2) + \frac{3O_1}{2}(1-4z^2)(4+\eta^2)\\
&\alpha_2 = O_0(5-24z^2+16z^4) + 6O_1(1-4z^2)\\
&\alpha_3 = 80\eta + 120\eta^3 + 10\eta^5 \quad \alpha_4 = 80\eta^2 + 40\eta^4 \quad \alpha_5 = 40\eta^3 + 5\eta^5\\
&\alpha_6 = 10\eta^4 \quad \alpha_7 = \eta^5 \quad \alpha_8 = 16 + 80\eta^2 + 30\eta^4
\end{aligned} \tag{20}$$

In order to calculate O_0 and O_1, it is necessary to recall that the Ocvirk number definition (Eq. (9)) includes the mean pressure, P_p, defined as

$$P_p = \frac{F}{2RL} \tag{21}$$

where the load-carrying capacity, F, is the magnitude of the load applied to the journal. If the system is equilibrated, then load has the same value as the force done by the lubricant to the journal. Consequently, F can be obtained integrating the fluid pressure field over the journal area (or bearing area, since $c \ll R$).

Another fact that has to be considered is that the film thickness is convergent in $0 < \Theta < 1$ and divergent in $1 < \Theta < 2$. The pressure

field given by Eq. (18) reaches positive values in the first region and negative ones in the second one. Given the limited capability of liquids to support negative pressures, the method frequently used to avoid the unrealistic sub-ambient pressures of the divergent zone when calculating F is to ignore them. This approach, known as the "π film" approach, is the most frequently used among analytical studies of JBs and it is also adopted in this work.

According to Fig. 1

$$F^2 = F_x^2 + F_y^2 \tag{22}$$

where

$$F_x = P_p LR\pi \int_{-1/2}^{1/2}\int_0^1 -p\cos(\pi\Theta)dz\,d\Theta \tag{23}$$

and

$$F_y = P_p LR\pi \int_{-1/2}^{1/2}\int_0^1 -p\sin(\pi\Theta)dz\,d\Theta \tag{24}$$

Replacing Eqs. (23) and (24) into Eq. (22) and combining with Eq. (21) gives

$$\frac{4}{\pi^2} = \left[\int_{-1/2}^{1/2}\int_0^1 -(p_0+\varepsilon p_1)\cos(\pi\Theta)dz\,d\Theta\right]^2 + \left[\int_{-1/2}^{1/2}\int_0^1 -(p_0+\varepsilon p_1)\sin(\pi\Theta)dz\,d\Theta\right]^2 \tag{25}$$

which can be expressed as

$$\frac{4}{\pi^2} = \left[\int_{-1/2}^{1/2}\int_0^1 p_0\cos(\pi\Theta)dz\,d\Theta\right]^2 + \left[\int_{-1/2}^{1/2}\int_0^1 p_0\sin(\pi\Theta)dz\,d\Theta\right]^2 + 2\varepsilon\left[\int_{-1/2}^{1/2}\int_0^1 p_0\cos(\pi\Theta)dz\,d\Theta\int_{-1/2}^{1/2}\int_0^1 p_1\cos(\pi\Theta)dz\,d\Theta\right] + 2\varepsilon\left[\int_{-1/2}^{1/2}\int_0^1 p_0\sin(\pi\Theta)dz\,d\Theta\int_{-1/2}^{1/2}\int_0^1 p_1\sin(\pi\Theta)dz\,d\Theta\right] + \mathcal{O}(\varepsilon^2) \tag{26}$$

O_0 and O_1 can then be obtained by solving the expressions of order-zero and order-ε in Eq. (26), respectively. This procedure gives

$$O_0 = \frac{4\kappa^2}{\eta\sqrt{4\eta^2+\pi^2\kappa^4 I_0^2}} \tag{27}$$

and

$$O_1 = \frac{2}{5}O_0\frac{3\eta^2(1+\eta^2)-2\pi^2\kappa^5 I_0[\beta+(2-7\eta^2)I_{s11}]}{\kappa\eta^2+\pi^2\kappa^5 I_0[\beta-(4+\eta^2)I_{s11}]} \tag{28}$$

with

$$\kappa = (1-\eta^2)\quad \beta = \eta(4I_{s12}+\eta I_{s13})\quad I_0 = \int_0^1 \frac{\sin^2(\pi\Theta)}{(1+\eta\cos(\pi\Theta))^3}d\Theta$$
$$I_{s11} = \int_0^1 \frac{-\sin^2(\pi\Theta)}{denom}d\Theta\quad I_{s12} = \int_0^1 \frac{\sin(\pi\Theta)\sin(2\pi\Theta)}{denom}d\Theta$$
$$I_{s13} = \int_0^1 \frac{\sin(\pi\Theta)\sin(3\pi\Theta)}{denom}d\Theta$$
$$denom = \alpha_3\cos(\pi\Theta)+\alpha_4\cos(2\pi\Theta)+\alpha_5\cos(3\pi\Theta)+\alpha_6\cos(4\pi\Theta)+\alpha_7\cos(5\pi\Theta)+\alpha_8 \tag{29}$$

The coefficients α_i are defined in Eq. (20).

The proposed method will be identified as the "P&O-perturbation" in the rest of the paper making reference to the fact the both pressure and Ocvirk number are expanded in order to extend the ISJB solution to describe finite length JBs.

For comparison reasons, two other perturbation expansions will be considered in the paper in which only the pressure is expanded. In one of them, p_0 and O_0 are the zero-order solution, like in the P&O-perturbation, and p_1 is calculated using O_0. This method, which will be identified as "P0-perturbation", produces a pressure solution that does not satisfy Eq. (26) but is of order ε. Furthermore, since the P0-perturbation solution is equivalent to that of the P&O-perturbation method with $O_1=0$, the comparison between these two solutions will clearly show the effect of O_1 in the proposed method. In the other case, the Ocvirk number is calculated introducing the expanded expression of the pressure $(p_0+\varepsilon p_1)$ in Eq. (26). This approach gives an O that is a function of ε and that will affect the zero-order term of the pressure, which will not match that of the ISJB solution when more than one term is considered. This method, which produces a pressure that is not of order ε, is equivalent to the one of Buckholz and Hwang [21] when only two terms are considered. The predictions of this last methodology will be identified as "P-perturbation".

4. Results

In the following sections, the results from the P&O-perturbation method are discussed and compared to the Ocvirk solution (ISJB solution), the numerical exact solution of Eq. (11), and the other two perturbation expansions previously commented. The comparison is carried out for L/D up to 1 and eccentricities between 0 and 1. The Ocvirk number is analyzed in the first section, followed by the discussion of the pressure profiles. Finally, the shear stress profiles and friction force results are analyzed.

4.1. Ocvirk number and load carrying capacity

Fig. 2 displays the value of the Ocvirk number as a function of the eccentricity ratio for four different values of L/D. The analytical results from the ISJB approximation (O_0) and the P-perturbation (O) and P&O-perturbation ($O_0+\varepsilon O_1$) methods are presented together with the numerical results of Eq. (11) and the results from Raimondi and Boyd [37]. The difference between Raimondi and Boyd's numerical solution and that of the full Reynolds equation arises from the boundary condition applied to pressure. Raimondi and Boyd used the Reynolds boundary condition [1,38] while the solution of Eq. (11) is obtained in this paper using Gümbel's (or π) boundary condition [38], which is also used in the perturbation methods.

As expected, all results agree in the limit of small aspect and eccentricity ratios. This can be seen in the data for $L/D=1/8$, where the curves are practically indistinguishable at all eccentricities, and in the data for larger aspect ratios in the region of $\eta\to 0$. As the aspect ratio increases, the curves separate as the eccentricity increases, the Ocvirk number calculated with the P&O-perturbation method being the one that follows more closely the numerical solution of Eq. (11). Additionally, it may be noticed that, agreeing with the hypotheses of the Ocvirk solution, its accuracy deteriorates when the Ocvirk number decreases. The distance between the ISJB and the P&O-perturbation solutions is due to the value of O_1. The Ocvirk number from the P-perturbation, which is always larger than $O_0+\varepsilon O_1$, also shows an improvement at low eccentricities, in the range of applicability of the Ocvirk solution, but gives non-real results outside this range.

Once the Ocvirk number has been calculated, the load-carrying capacity, F, can be obtained from Eq. (9) as follows:

$$F = 2\frac{\mu LU}{O}\left(\frac{R}{c}\right)^2\left(\frac{L}{R}\right)^2 \tag{30}$$

where O is the Ocvirk number given by different solutions in Fig. 2. In the case of the P&O-perturbation, an analytical solution

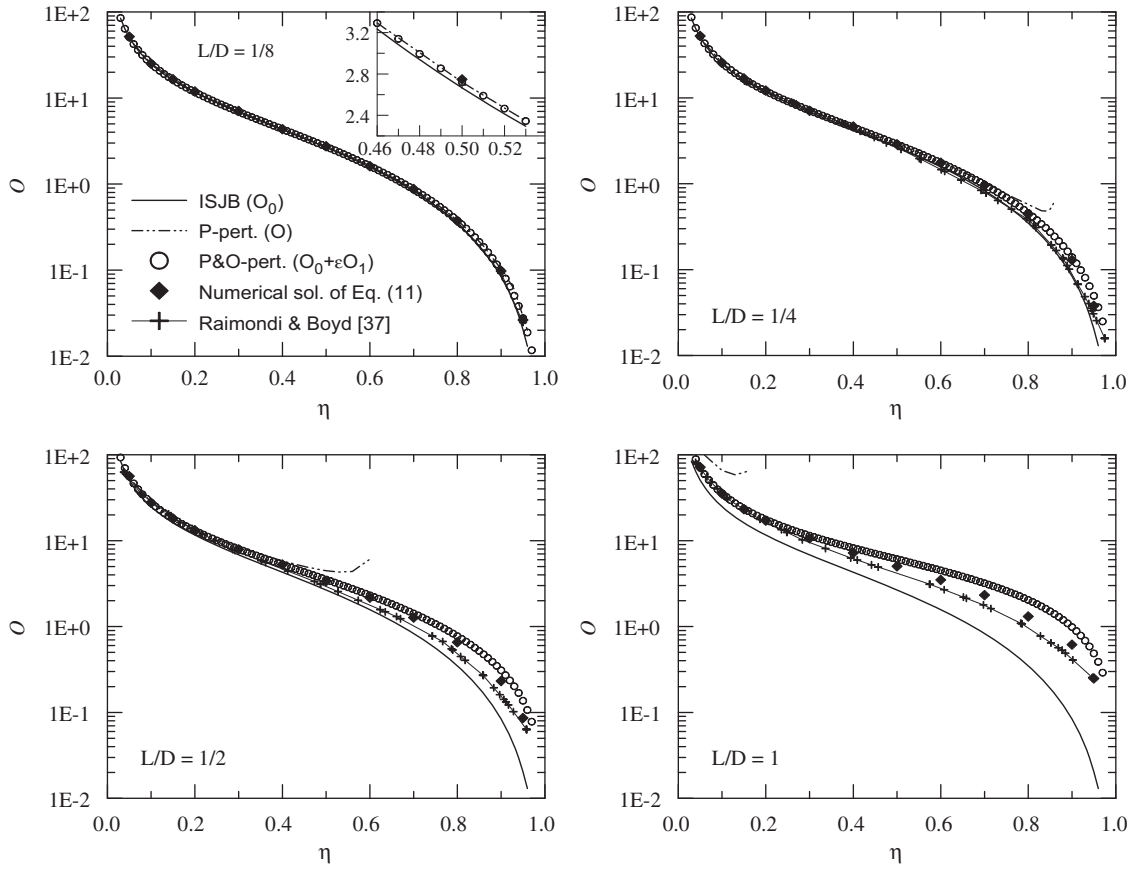

Fig. 2. Ocvirk number as a function of eccentricity ratio for different aspect ratios.

of F may be obtained using $O=O_0+\varepsilon O_1$ and the expressions of O_0 and O_1 are given by Eqs. (27) and (28).

4.2. Pressure profiles

Fig. 3 displays the values of $p_0(\Theta)$ and $p_1(\Theta)$ as a function of eccentricity ratio calculated with Eqs. (27) and (28) at $z=0$. p_0 is also the Ocvirk solution and the zero-order term of the P0-perturbation method. This function has a sinusoidal dependency with the azimuthal position when $\eta \to 0$ (as a result of the way the dimensionless pressure has been defined) and displays a maximum value that gradually shifts towards the region of minimum gap as the eccentricity increases. The first-order solution of the Reynolds' equation obtained with the P&O-perturbation method gives curves of $p_1(\Theta)$ that tend to increase the zero-order solution at small angles and to reduce it at large angles. As expected, this effect is small at small eccentricities and gets dramatic as the eccentricity increases. The predicted pressure $(p_0+\varepsilon p_1)$ will be slightly larger than in the ISJB for $\Theta < 0.4$ regardless of the aspect and eccentricity ratios (for $L/D < 1$). At larger angles, the larger the eccentricity, the smaller the aspect ratio (and vice versa) that will keep the corrective term to be of smaller order of magnitude than the zero-order pressure term. For certain combinations of aspect and eccentricity ratios, the pressure may become negative near the minimum gap.

As an example, Fig. 4 shows the pressure profiles predicted by the ISJB approximation and the different perturbation methods as a function of the azimuthal direction, calculated at $z=0$

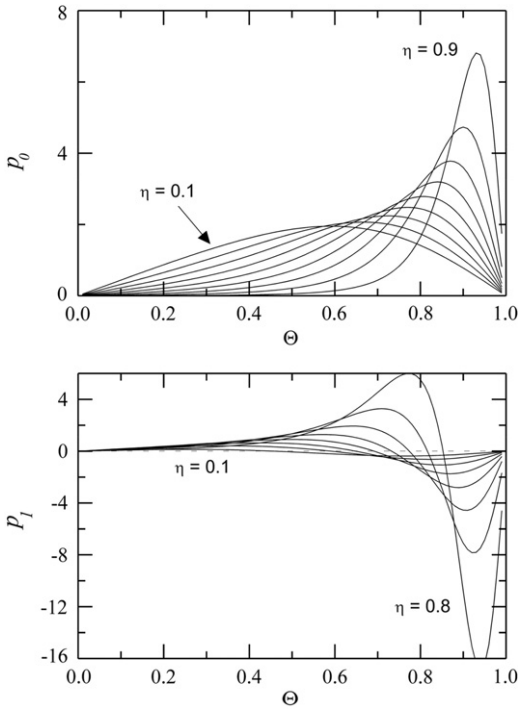

Fig. 3. Dimensionless zero- and first-order functions of the expanded pressure according to the proposed P&O-perturbation method at $z=0$. The curves are presented with steps of 0.1 in the value of eccentricity.

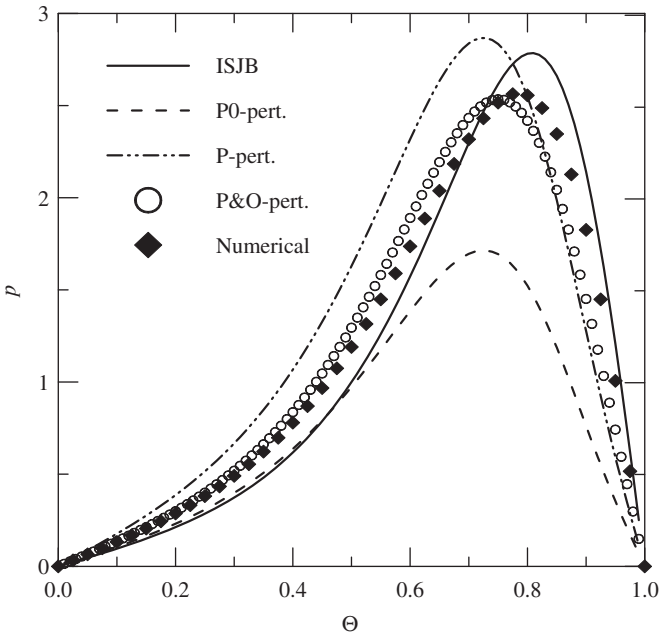

Fig. 4. Dimensionless pressure profiles predicted by the different methods at $z=0$ for $L/D=0.5$ and $\eta=0.5$.

and the selected conditions $L/D=0.5$ and $\eta=0.5$. The exact solution of Eq. (11), obtained numerically, is also displayed in that plot.

As it may be appreciated, all approximate solutions are qualitatively correct although the prediction of the P&O-perturbation is the one closest to the numerical solution, at least up to the vicinity of the maximum pressure. This method, although locates p_{max} a little before the position given by the numerical method (difference in $\Theta_{max}\approx 0.03$), is the one that gives the closest value (underpredicts the peak pressure by just 1.3%). The ideal Ocvirk solution, on the other hand, overestimates the maximum pressure by 8.6% and locates it after its position (difference with respect to the numerical solution of $\Theta_{max}\approx 0.03$). The P0-perturbation method, which uses O_0 in the calculation of p_1, largely underestimates the peak pressure by 33% because p_1 reaches relatively large and negative values. The P-perturbation solution, on the other hand, overestimates the peak pressure by 12%. Both these methods place the maximum pressure before its location (difference in $\Theta_{max}\approx 0.05$). The results displayed in Fig. 4 show that the P&O-perturbation method is the one that, in general, better captures the physics of the flow, at least at the aspect and eccentricity ratios considered in this figure. This method predicts a pressure field that practically matches the exact solution up to $\Theta=0.4$, stays the closest up to $\Theta\cong 0.6$, and it is not far away from it at larger angles. When the sum of the square differences between the pressure predicted by the different methods and the numerically calculated are considered for $0<\Theta<1$, the smallest value is that of the P&O-perturbation method followed by the ISJB approximation.

A more complete analysis of the capabilities and limitations of the proposed method can be done from Fig. 5. This figure displays the pressure profiles calculated at $z=0$ as a function of journal aspect ratio (for $\eta=0.5$) and eccentricity ratio (for $L/D=0.5$) at three different azimuthal positions. Within the analyzed ranges, the results show that, the zero-order solution matches the exact numerical results at all azimuthal positions only at very small aspect and eccentricities ratios ($L/D<0.1$ and $\eta<0.05$). For $\eta=0.5$, the P0-perturbation method makes an improvement over the Ocvirk solution only at small values of Θ, regardless the aspect ratio (Fig. 5, left), while for $L/D=0.5$, it worsens the ISJB solution at small eccentricities for all Θs and at practically all eccentricities ratios for $\Theta>0.5$, always underestimating the pressure. The P-perturbation method, on the other hand, gives good results only at low aspect ($L/D<0.3$) and eccentricities ($\eta<0.2$-0.3) ratios, regardless of the angular position. Outside these ranges, it overestimates the pressure to finally diverge to non-real values. Then, according to Fig. 5, the ISJB approximation gives, in general, better predictions of $p(\Theta)$ than the P- and P0-perturbation methods, at least at the selected conditions. The P&O-perturbation, on the other hand, largely improves the predictions of the ISJB method. The pressure calculated with the proposed method agrees with the numerical results in larger ranges of aspect and eccentricity ratios and produces realistic values outside those ranges. Furthermore, $p(\Theta)$ practically matches exactly the numerical results for $L/D<0.35$ at all Θs (for $\eta=0.5$) and for small Θ's at all η's and for $\eta<0.35$ at larger Θs ($L/D=0.5$).

4.3. Friction force

Another useful variable to analyze is the shear stress. The dimensionless shear stress at the moving wall is defined as

$$T=-\left.\frac{\partial u}{\partial y}\right|_h=\frac{\tau|_h c}{\mu U} \tag{31}$$

which corresponds to the integration of the dimensionless Θ-Direction Momentum Balance at the moving wall, after applying no-slip boundary conditions, that is

$$T=-\left.\frac{\partial u}{\partial y}\right|_h=-\left(\frac{1}{\pi O}\left(\frac{L}{R}\right)^2\frac{\partial p}{\partial\Theta}\frac{h}{2}+\frac{1}{h}\right) \tag{32}$$

Fig. 6 shows the shear stress profile at the moving wall calculated at the same conditions than the pressure profiles of Figs. 4 and 5. The displayed results demonstrate that the capabilities and limitations of the proposed method to predict both, pressure and shear stress profiles, are the same. As expected, the zero-order solution of the Reynolds equation describes the behavior of very short JBs and small eccentricities. The P0- and P-perturbation methods give the same shear stress profiles, at least in the range of real values of O of the P-perturbation. This is because $p(\Theta)$ has the same analytical expression in both cases ($p=p_0+\varepsilon p_1\sim O$), differing only in the value of O. According to Fig. 6, these methods give values of T that approach those of the numerical results in larger ranges of aspect and eccentricity ratios than the ISJB method. The first-order solution obtained with the proposed P&O-perturbation method matches the exact numerical results up to L/D of at least 0.4 and improves the matching outside this range at practically all tested conditions.

The friction force, F_f, which corresponds to the integration of the fluid shear stress over the journal area, can be also defined as the product of a friction coefficient, f, and the load-carrying capacity,

$$F_f=\int_0^2\int_{-1/2}^{1/2}\tau|_h\pi RL\,d\Theta\,dz=fF \tag{33}$$

Accordingly, a friction coefficient, $f(R/c)(L/R)^2$, can be obtained combining Eq. (33) with Eq. (30) and considering $\tau=-(\mu U/c)(\partial u/\partial y)$ and that, according to the π film hypothesis, in the divergent zone of the fluid film, $1<\Theta<2$, a Couette type of flow exists (linear velocity profile). That is,

$$f\frac{R}{c}\left(\frac{L}{R}\right)^2=\frac{1}{2}\pi O\int_0^1\int_{-1/2}^{1/2}\left.\frac{\partial u}{\partial y}\right|_h d\Theta\,dz+\frac{1}{2}\pi O\int_1^2\int_{-1/2}^{1/2}\frac{1}{h}d\Theta\,dz \tag{34}$$

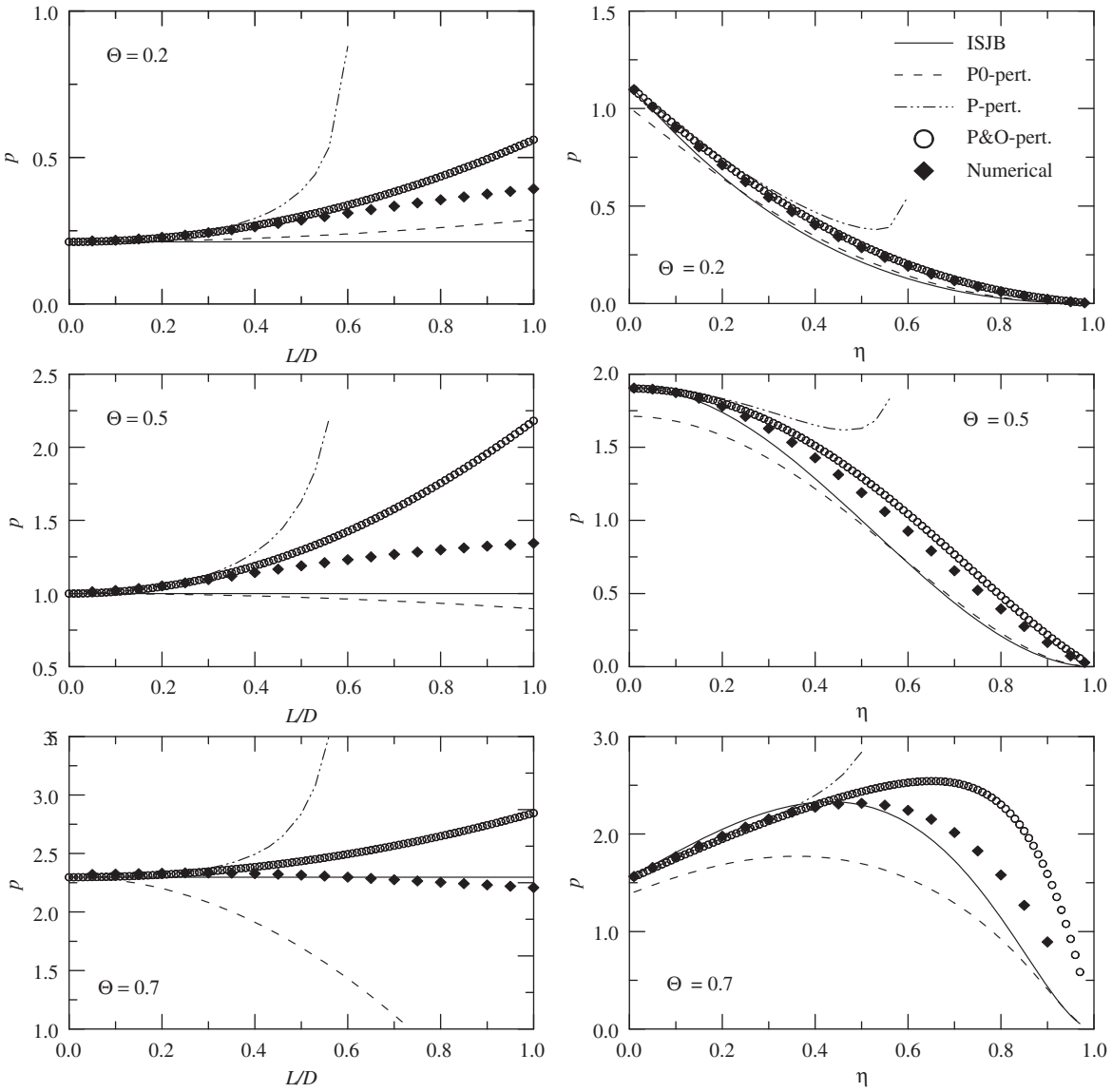

Fig. 5. Dimensionless pressure profiles at three different tangential positions as a function of dimensionless length (left, $\eta=0.5$) and eccentricity (right, $L/D=0.5$).

which can be combined with Eq. (32) to give the following expression:

$$f\frac{R}{c}\left(\frac{L}{R}\right)^2=\varepsilon\int_0^1\int_{-1/2}^{1/2}h\frac{\partial p}{\partial\Theta}d\Theta\,dz+\frac{1}{2}\pi O\int_0^2\int_{-1/2}^{1/2}\frac{1}{h}d\Theta\,dz \qquad (35)$$

The dominant term in Eq. (35) is the second integral-term in the right-hand side (Couette flow), which establishes that the factor f R/c is of order $(R/L)^2$. Furthermore, this integral-term (evaluated with O_0) corresponds to the prediction of $f(R/c)(L/R)^2$ of the ISJB approximation ($L/D\to 0$) and to the zero-order term of the P0- and P&O-perturbations (using O_0) and of the P-perturbation (using O). The corrective first-order terms of the P0- and P-perturbations are given by the first integral-term evaluated using the zero-order expression of the pressure. The P&O-perturbation method contemplates an additional first-order term, the one obtained from replacing O by $(O_0+\varepsilon O_1)$ in the second integral.

Fig. 7 displays the friction coefficient as a function of eccentricity for four different aspect ratios. The figures also include the exact numerical solution of the Reynolds equation and the results from Raimondi and Boyd. At $L/D=1/8$, the predicted friction coefficients are practically indistinguishable at all eccentricities. The same occurs at low eccentricities and larger aspect ratios although, as expected, the range of agreement of the predictions decreases as L/D increases. The first-order term in the P0-perturbation expansion (generated by the azimuthal variation of p) slightly increases the value of the friction coefficient, which is still too low compared with the exact value (mainly at large L/D). The P-perturbation, extends the range of accuracy of the ISJB, mainly up to aspect ratios of about 0.5, but predicts non-real results at values of eccentricity that abruptly decrease as the aspect ratio increases. The best predictions are those of the P&O-perturbation method, that fall extremely close to the exact solutions. The accuracy of this method in the calculation of the friction coefficient extends up to $L/D=1$ and ε practically 1. Undoubtedly, the P&O-perturbation, with the expansion of both, the pressure and the Ocvirk number (which is a dimensionless mean pressure), is the one that better captures the physics of the JB flow.

Finally, following a criteria similar to the one of Pandazaras and Petropoulos [39], Fig. 8 presents iso-operational curves using the Ocvirk number as the operational parameter. The figure displays eccentricity and friction coefficient as a function of aspect ratio at $O=1$, 10, and 100. Fig. 8(left) shows that different

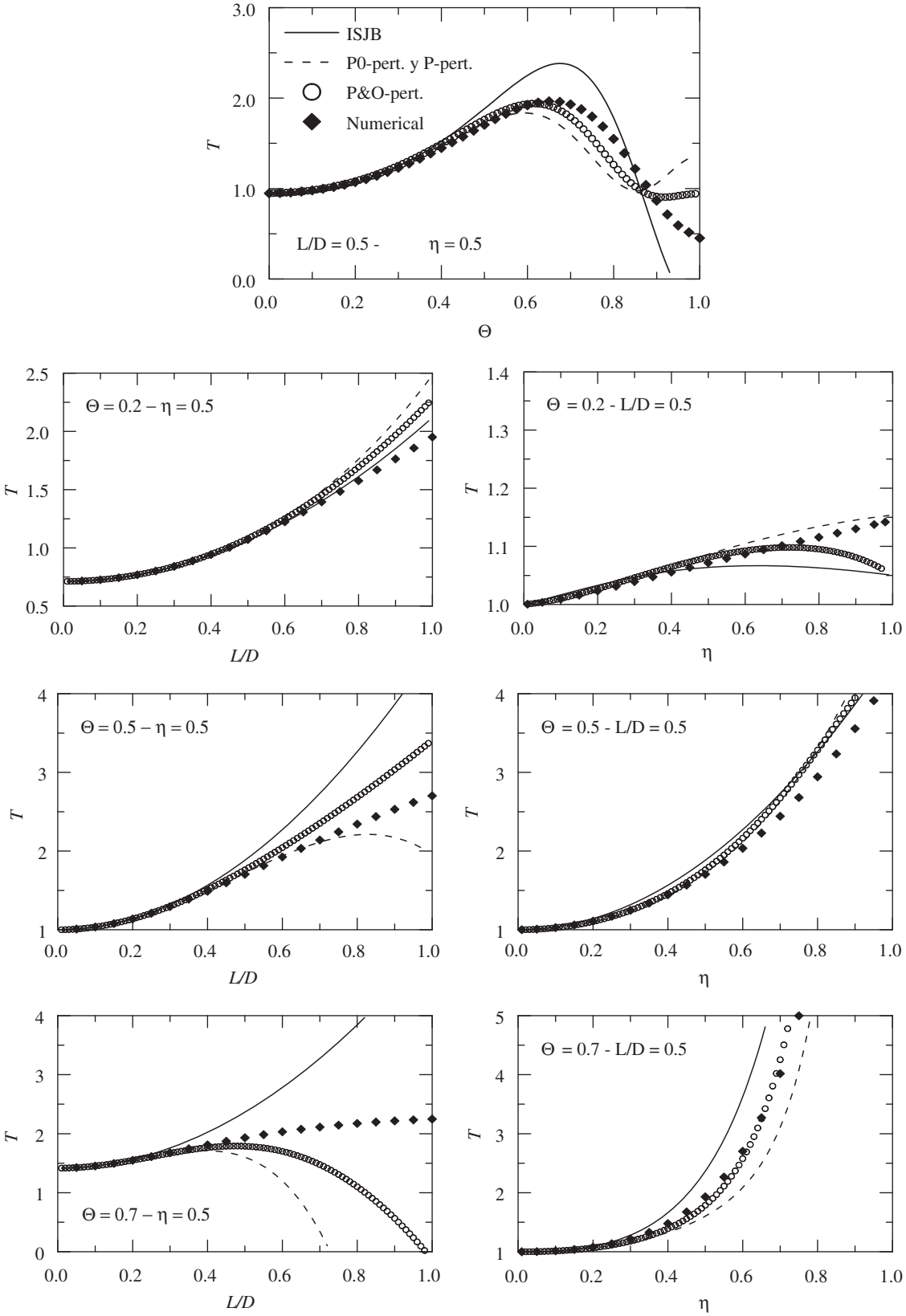

Fig. 6. Dimensionless shear stress profiles as a function of tangential position (top, $\eta=0.5$, $L/D=0.5$), dimensionless length (left, $\eta=0.5$) and eccentricity (right, $L/D=0.5$).

values of *O* determine different ranges of eccentricity that should be used for the range of aspect ratio considered in this work. Similarly, Fig. 8(right) shows that those values of *O* determine different ranges of friction coefficient. As expected, as the Ocvirk number decreases, the eccentricity increases and the friction coefficient decreases.

The figure shows that, at low *L*/*D*, all curves match at all Ocvirk numbers. However, as the aspect ratio increases, the

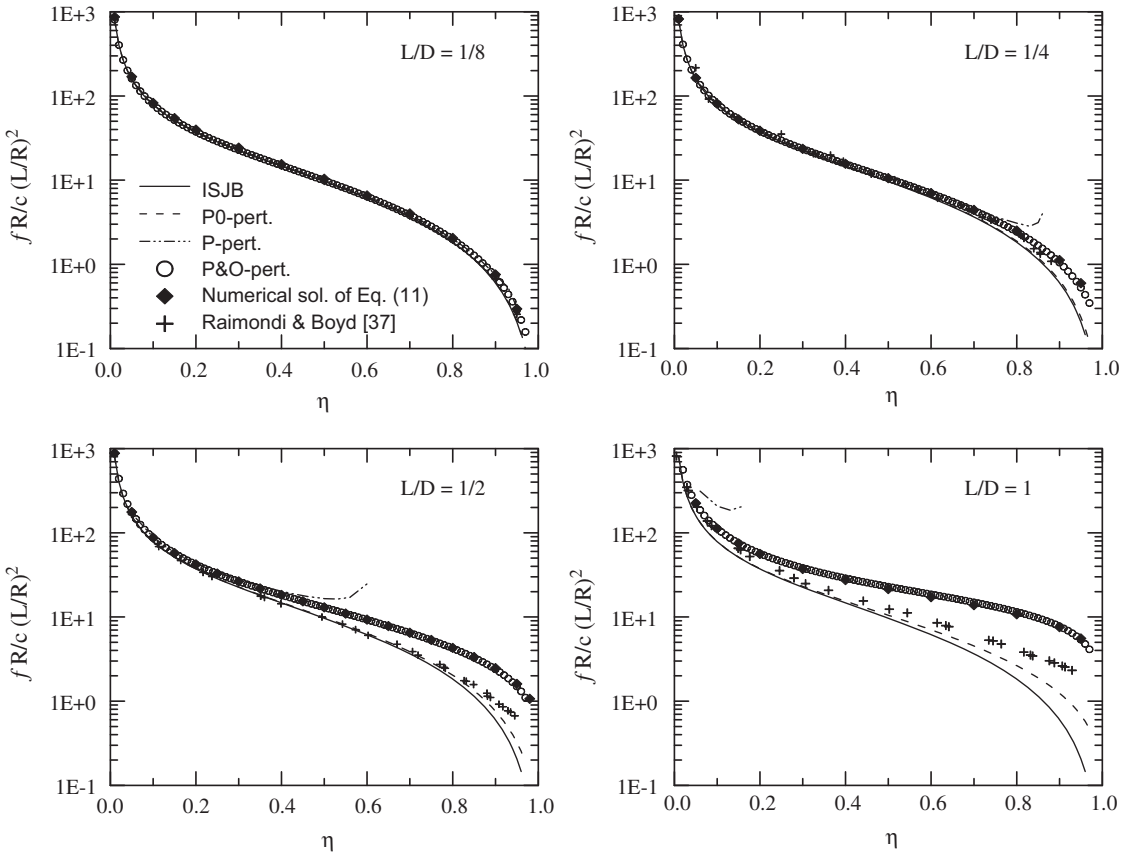

Fig. 7. Dimensionless friction coefficient as a function of eccentricity ratio for different aspect ratios.

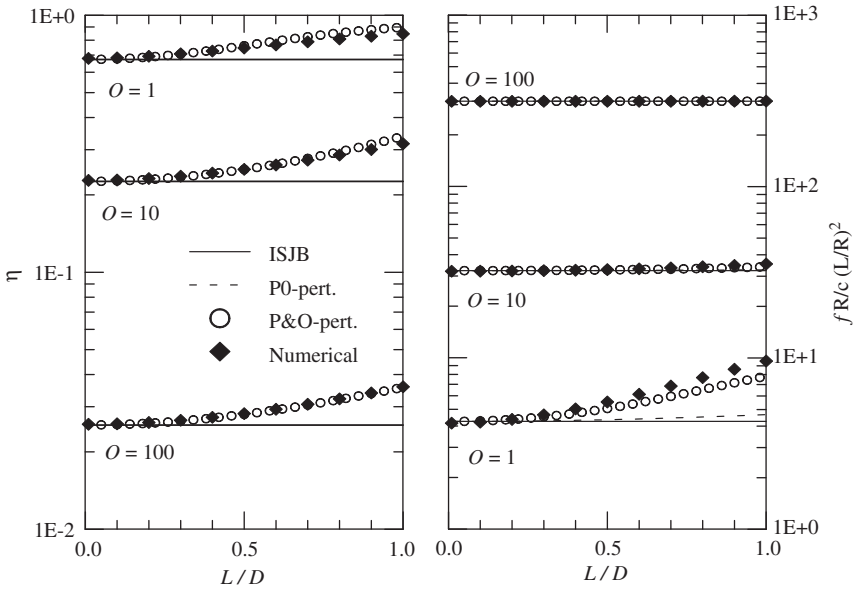

Fig. 8. Dimensionless eccentricity (left) and friction coefficient (right) as a function of aspect ratio for three constant Ocvirk numbers.

operational curves separate. The ISJB approximation ($L/D \to 0$) predicts constant values for each O while the other techniques display curves with values that increase as L/D increases. It can also be appreciated that, the lower the value of O, the larger the separation. In agreement with the results already displayed in the previous figures, the P&O-perturbation method is the one that follows closely the numerical solution of the Reynolds equation.

5. Conclusions

An analytical tool to perform finite journal bearing calculations is introduced. The novelty of the proposed regular perturbation method lies in that both, the pressure and the Ocvirk number, are expanded. This idea is supported by the fact that the Ocvirk number is a dimensionless mean pressure and that the order of magnitude of the pressure varies with aspect ratio. The square of

the aspect ratio is then used as the perturbation parameter. Pressure and shear-stress, as well as the Ocvirk number and the friction coefficient (total friction force over load-carrying capacity) were calculated and analyzed as a function of azimuthal position, if applies, and aspect and eccentricity ratios.

The zero-order solution of the proposed perturbation method corresponds to the ISJB approximation ($L/D \to 0$). This approximation correctly describes the behavior of short journal bearings up to approximately the following limits: $\eta < 1$ for $L/D = 1/8$; $\eta < 0.6$ for $L/D = 1/4$; $\eta < 0.2$ for $L/D = 1/2$; and $\eta \to 0$ for $L/D = 1$. The first-order solution of the proposed method extends the limits up to $\eta \sim 0.9$ for $L/D = 1/4$; $\eta \sim 0.6$ for $L/D = 1/2$; and $\eta \sim 0.4$ for $L/D = 1$. In the case of variables that correspond to the integration of pressure or stress fields, like friction coefficient and load-carrying capacity (and even the Ocvirk number itself) the improvement in the range of accuracy is larger. The friction coefficient is, for example, very well described even for bearings with aspect ratio up to 1 and medium to high eccentricities.

Consequently, the treatment of the Ocvirk number as an expansible variable produces noticeable improvements in the analytical description of the flow fields of journal bearings, and even more remarkable ones in the calculations of load-carrying capacity and friction coefficient.

References

[1] Hamrock BJ, Schmid SR, Jacobson BO. Fundamentals of fluid film lubrication. 2nd ed. New York: Marcel Dekker, Inc.; 2004.
[2] Reynolds O. On the theory of lubrication and its application to Mr. Beauchamp Tower's experiments, including an experimental determination of the olive oil. Phil Trans Roy Soc 1886;177:157–234.
[3] Pinkus O. Theory of hydrodynamic lubrication. New York: McGraw Hill; 1961.
[4] Fuller DD. Theory and practice of lubrication for engineers. New York: John Wiley and Sons; 1961.
[5] Dubois GB, Ocvirk FW. Analytical derivation of short bearing approximation for full journal bearings. NACA Report 1953;1157.
[6] Sommerfeld A. The hydrodynamic theory of lubrication friction. Zs Math Phys 1904;50(1,2):97–155.
[7] Barrero Ripoll A, Perez-Saborid Sanchez-Pastor M. Fundamentos y Aplicaciones de la Mecánica de Fluidos. Madrid: McGraw Hill; 2005.
[8] Ling F. Asymptotic analyses in isothermal fluid film lubrication theories. SIAM Rev 1986;28(3):343–66.
[9] Capriz G, Cimatti G. On some singular perturbation problems in the theory of lubrication. Appl Math Opt 1978;4:285–97.
[10] Nayfeh A. Perturbation methods. New York: John Wiley & Sons; 1973.
[11] CHT Pan. On asymptotic analysis of gaseous squeeze-film bearings. ASME J Lubr Technol 1967;89:245–53.
[12] Gross WA, Zachmanoglou EC. Perturbation solutions for gas-lubricating films. ASME J Basic Eng 1961;83:139–44.
[13] Di Prima RC. Asymptotic methods for an infinitely long slider squeeze-film bearing. ASME J Lubr Technol 1968;90:173–83.
[14] Di Prima RC. Asymptotic methods for an infinitely long step slider squeeze bearing. ASME J Lubr Technol 1973;95:208–16.
[15] Di Prima RC. Higher order approximations in the asymptotic solution of the Reynolds equation for slider bearings at high bearing numbers. ASME J Lubr Technol 1969;91:45–51.
[16] Schmitt JA, Di Prima RC. Asymptotic methods for an infinite slider bearing with a discontinuity in film slope. ASME J Lubr Technol 1976;98:446–52.
[17] Eckhaus W, De Jager EM. Asymptotic solutions of singular perturbation problems for linear differential equations of elliptic type. Arch Rational Mech Anal 1966;23:26–86.
[18] Grasman J. On singular perturbation and parabolic boundary layers. J Eng Math 1968;2:163–72.
[19] Di Prima RC. Asymptotic methods for a general finite width gas slider bearing. ASME J Lubr Technol 1978;100:254–60.
[20] Schuss Z, Etsion I. On the solution of lubrication problems involving narrow configurations. ASLE Trans 1981;24(2):186–90.
[21] Buckholz RH, Hwang B. The accuracy of short bearing theory for Newtonian lubricants. ASME J Tribol 1986;108:73–9.
[22] Rohde SM, Li DFA. Generalized short bearing theory. ASME J Lubr Technol 1980;102:278–82.
[23] Buckholz RH, Lin J, Pan CHP. On the role of axial edge effects and cavitation in lubrication for short journal bearings. ASME J App Mech 1984;52(2):267–73.
[24] Tayler AB. A uniformly valid asymptotic solution of Reynolds's equation: the finite journal bearing with small clearance. Proc Roy Soc A 1968;305(1482):345–61.
[25] Di Prima RC, Stuart JT. Flow between eccentric rotating cylinders. ASME J Lubr Technol 1972;94:266–74.
[26] Wannier GH. A contribution to the hydrodynamics of lubrication. Quart Appl Math 1950;8:1–32.
[27] Kamal MM. Separation in the flow between eccentric rotating cylinders. ASME J Basic Eng 1966;88:717–24.
[28] Wood WW. The asymptotic expansions at large Reynolds numbers for steady motion between non-coaxial rotating cylinders. J Fluid Mech 1957;3:159–75.
[29] Myllerup CM, Hamrock BJ. Perturbation approach to hydrodynamic lubrication theory. ASME J Tribol 1994;116:110–8.
[30] Fuller DD. Fluid film bearings. In: Avallone EA, Baumeister III T, editors. Marks' standard handbook for mechanical engineers. 9th ed. New York: McGraw Hill; 1987. p. (8)-116-31.
[31] Rezvani MA, Hahn EJ. Limitations of the short bearing approximation in dynamically loaded narrow hydrodynamic bearings. ASME J Tribol 1993;115(3):544–9.
[32] Hirani H, Athre K, Biswas S. Dynamically loaded finite length journal bearings: analytical method of solution. ASME J Tribol 1999;121(4):844–52.
[33] Bastani Y, de Queiroz MA. New analytic approximation for the hydrodynamic forces in finite-length journal bearings. ASME J Tribol 2010;132(1). (014502-1-9).
[34] McHugh JD. Learning from unexpected consequences-the roots of tribology. Lubr Eng 1999;55(7):33–9.
[35] San Andrés L Static load performance of plain journal bearings. Class notes on modern lubrication. College Station (TX): Texas A&M University; 2006.
[36] Bender CM, Orszag SA. Advanced mathematical methods for scientists and engineers. New York: McGraw Hill; 1978.
[37] Raimondi A, Boyd JA. Solution for the finite journal bearing and its application to analysis and design, parts I, II, and III. ASLE Trans 1958;1(1):159–209.
[38] Mori H, Yabe H, Fujita Y. On the separation boundary condition for fluid lubrication theories of journal bearings. ASLE Trans 1968;11(3):196–203.
[39] Pandazaras C, Petropoulos G. Tribological design of hydrodynamic sliding journal bearings. Formulating new functional charts. Ind Lubr Tribol 2005;57:4–11.